Rev.Adv.Mater.Sci. 18(2008) 77-80

CRYSTALLIZATION OF $Cu_{54}Ni_6Zr_{22}Ti_{18}$ AMORPHOUS ALLOY DURING ISOTHERMAL ANNEALING IN SUPERCOOLED LIQUID REGION

E. S. Park[1], M. Y. Huh[1], J. H. Lee[1], H. J. Kim[2] and J. C. Bae[2]

[1]Division of Materials Science and Engineering, Korea University, Seoul, 136-701, Korea
[2]R&D Division for Bulk Amorphous & Nano Materials, Korea Institute of Industrial Technology, Inchon 406-130, Korea

Received: March 29, 2008

Abstract. The crystallization of $Cu_{54}Ni_6Zr_{22}Ti_{18}$ amorphous alloy during isothermal annealing in the supercooled liquid region was investigated by thermal and structural examinations. At the early stage of annealing, the amorphous alloy was first decomposed into copper-rich and copper-poor amorphous phases. Crystalline $Cu_{51}Zr_{14}$ first formed in copper-rich area and subsequently Cu-Zr and Cu-Ti intermetallic crystals formed with increasing annealing time.

1. INTRODUCTION

Upon annealing above the glass transition temperature (T_g), bulk metallic glass (BMG) alloys crystallize in two different ways. In some BMG alloys, the crystallization is initiated by the precipitation of nano-crystals in heterogeneous nucleation sites (e.g. [1]). Some other BMG alloys first decompose into two amorphous phases having slightly different compositions and the crystallization takes places in the decomposed amorphous phases (e.g. [2]). The formation of amorphous mixture prior to the crystallization was studied in detail elsewhere [3]. However, the sequence of the crystallization processes in the decomposed amorphous phases during isothermal annealing has seldom been reported.

In the present work, the formation of crystalline phases from the decomposed amorphous phases in $Cu_{54}Ni_6Zr_{22}Ti_{18}$ during isothermal annealing at 723K was investigated by thermal and structural examinations.

2. EXPERIMENTAL PROCEDURE

BMG powder of $Cu_{54}Ni_6Zr_{22}Ti_{18}$ was produced by a high pressure gas atomization. To produce the rod sample, BMG powder was consolidated by spark plasma sintering (SPS) [4]. The thermal behavior was determined by differential scanning calorimetry (DSC). Structural characterization was carried out in the X-ray diffractometry (XRD) and high resolution transmission electron microscope (HRTEM). The micro-composition analysis was performed by nano-beam energy dispersive spectroscopy (EDS) and electron energy loss spectroscopy (EELS).

3. RESULTS AND DISCUSSION

As addressed previously, the present sample was produced by atomization of BMG powder and consolidation of this powder using SPS. The thermal behavior of the BMG sample with increasing isothermal annealing time at 723K is shown in DSC curves in Fig. 1. The glass transition temperature

Corresponding author: M. Y. Huh, e-mai: myhuh@korea.ac.kr

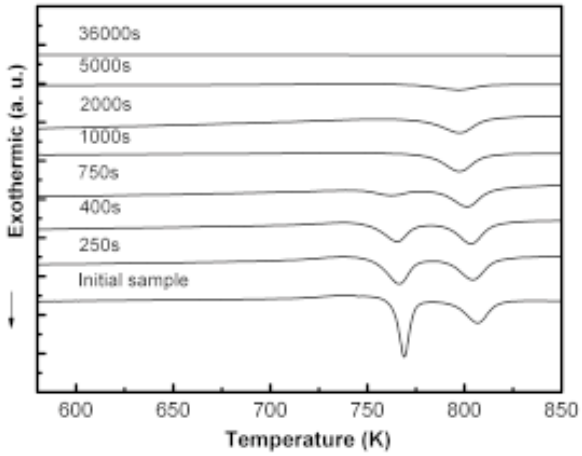

Fig. 1. DSC curves showing thermal behavior of BMG alloy with increasing annealing time at 723K.

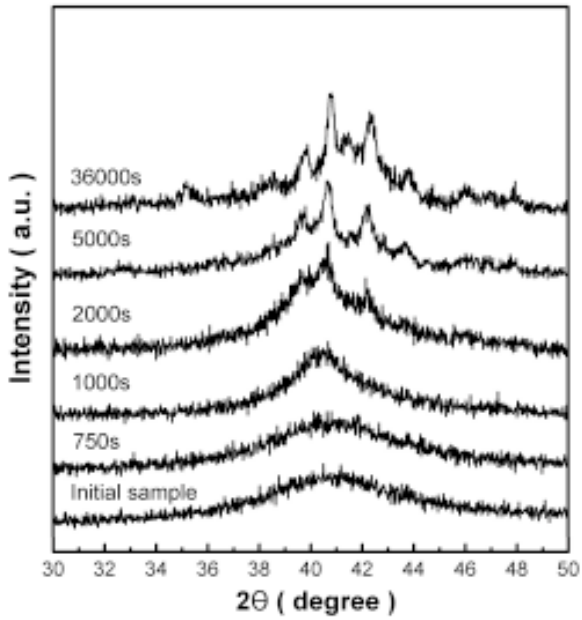

Fig. 2. Variations of XRD pattern with increasing annealing time at 723K.

(T_g) of the initial sample was 712K. DSC curve of the initial sample displays two exothermic peaks of the crystallization temperatures (T_x) at 763K and 790K, implying a two-step crystallization process. The first exothermic peak decreases with increasing annealing time until 750 s and completely disappears in the samples annealed longer than 1000 s. It is noted that the temperatures T_g and T_x gradually varies with increasing annealing time, reflecting structural and compositional changes of BMG alloy. After annealing for 36000 s, the sample displays no thermal response in the DSC curve.

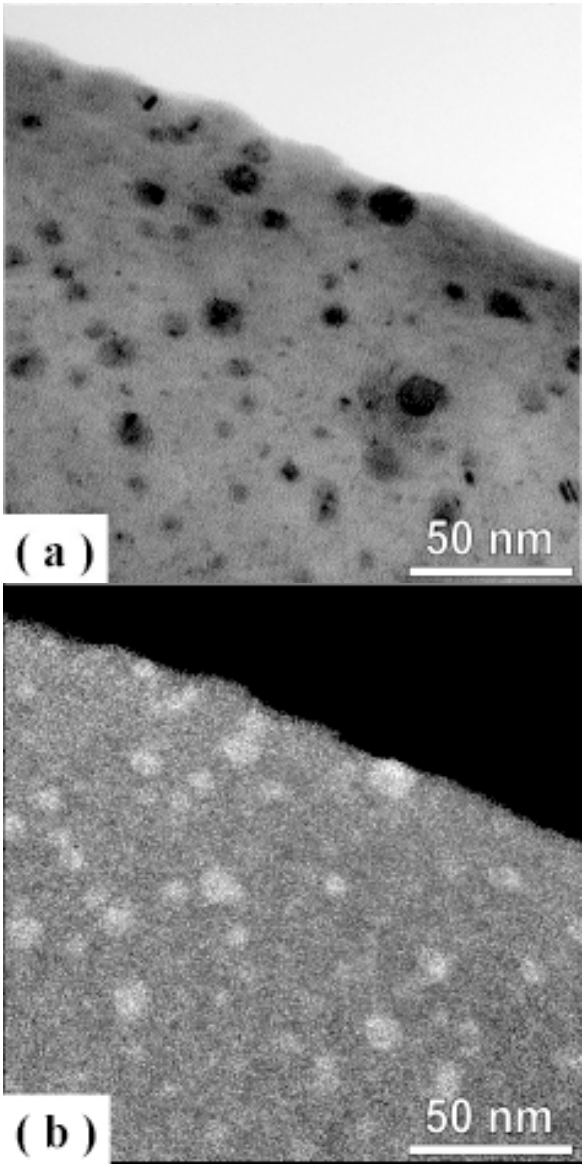

Fig. 3. Microstructure observed in the sample annealed for 750 s at 723K. (a) Bright field image recorded by EFTEM, (b) Cu mapping image recorded by EELS.

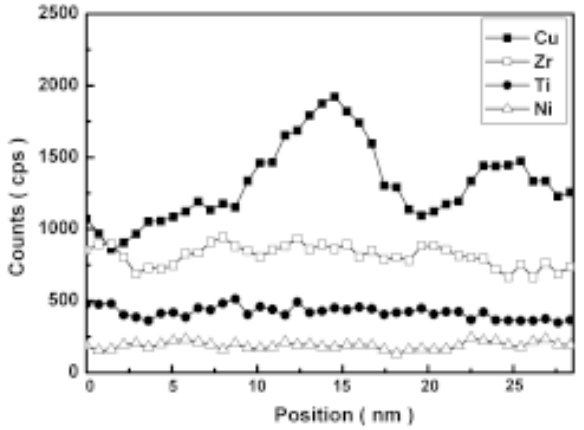

Fig. 4. Variations of characteristic X-ray counts of Cu, Zr, Ti and Ni along a line segment of ~30 nm. A dark-contrast spot in Fig. 3a was positioned at the center of the analyzed line segment.

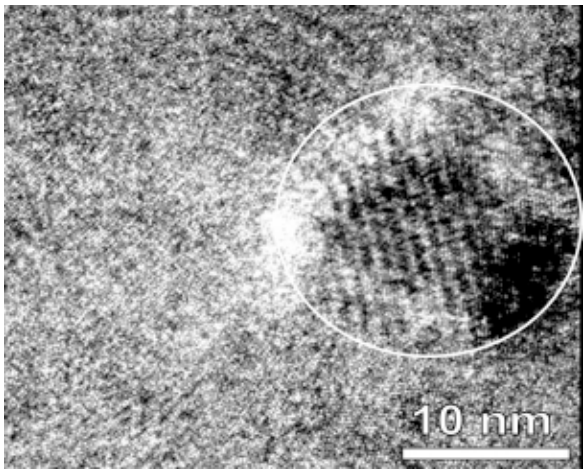

Fig. 5. HRTEM image observed in the sample annealed for 2000 s at 723K.

Fig. 2 shows variations of the XRD pattern of the present BMG alloy with increasing annealing time at 723K. The samples annealed shorter than 750 s display the XRD pattern with a broad hump that is typically found in an amorphous phase. After annealing for 1000 s, the amorphous hump becomes somewhat narrower and higher. However, crystalline peaks were hardly recognized in this XRD pattern. Peaks from crystalline phases mostly from $Cu_{51}Zr_{14}$ were first observed after annealing for 2000 s. With increasing annealing time to 5000 s, intensity of crystalline peaks increases and peaks from Cu-Ti intermetallic crystals are newly found. A large number of crystalline peaks is observed in the sample annealed for 36000 s in which peaks from $Cu_{51}Zr_{14}$, Cu_8Zr_3, $Cu_{10}Zr_7$, CuTi, Cu_4Ti_3 and Cu_3Ti_2 are identified.

The samples annealed to 750 s exhibited no change in the XRD pattern. Furthermore, these samples depicted still two characteristic exotherms in the DSC curve as the initial sample. Careful HRTEM observations disclose that no crystalline phases developed after annealing for 750 s. However, the microstructure recorded by HRTEM showed that annealing for 750 s led to the formation of two distinct areas displaying dark and bright contrasts which were not found in the initial amorphous microstructure. In order to examine the formation of this contrast, energy filtered transmission electron microscopy (EFTEM) coupled with EELS is employed to obtain the elemental mappings image in an atomic scale. As shown in Fig. 3a, the bright field image recorded by EFTEM clearly displays the spots with dark contrast having various sizes ranging from a few nm to 15 nm in the sample annealed at 723K for 750 s. The Cu mapping image in Fig. 3b reveals that Cu atoms are segregated in the dark contrast spots in Fig. 3a. Accordingly, it is evident that isothermal annealing of the present alloy first gave rise to the decomposition of the original amorphous phase into two amorphous phases different in composition, i.e. Cu-rich and Cu-poor phases.

To further examine the variation of the chemical composition in the decomposed phases, nanobeam EDS equipped on STEM was carried out along a line segment of ~30 nm in the sample annealing for 750 s. Fig. 4 shows the characteristic X-ray counts measured as a function of sample positions, where a dark contrast spot was positioned at the center of the analyzed line segment. A large variation in the composition, Cu in particular, along the scanned line further confirms that the Cu-enriched regions formed as a result of Cu diffusion.

Fig. 5 shows HRTEM image of the sample annealed for 2000 s. The area with a dark contrast contains nano-crystals of hexagonal $Cu_{51}Zr_{14}$ in which {410} lattice planes are identified. In this microstructure, clear lattice planes were seldom observed in the bright area. This result indicates that the crystallization first occurred in the copper-rich amorphous phase decomposed from the initial BMG alloy.

4. CONCLUSIONS

The crystallization of $Cu_{54}Ni_6Zr_{22}Ti_{18}$ amorphous alloy during isothermal annealing at 723K was studied. At the early stage of annealing, the initial BMG alloy was decomposed into copper-rich and copper-poor amorphous phases. Nano-crystals of $Cu_{51}Zr_{14}$ firstly formed in the copper-rich amorphous phase and subsequently Cu-Zr and Cu-Ti intermetallic crystals developed with increasing annealing time.

ACKNOWLEDGEMENTS

This work is supported by the next generation new technology development program of ministry of commerce, industry, and energy in Korea.

REFERENCES

[1] D.R. Allen, J.C. Foley and J.H. Perepezko // *Acta Mater.* **46** (1998) 431.
[2] S.C. Glade, J.F. Löffler, S. Bossuyt and W.L. Johnson // *J. Appl. Phys*. **89** (2001) 1573.
[3] E. Pekarskaya, J.F. Löffler and W.L. Johnson // *Acta Mater.* **51** (2003) 4045.
[4] M.Y. Huh, E.S. Park, H.J. Kim and J.C. Bae // *Mater. Sci. Eng. A*, **449-451** (2007) 916.